Data-driven Sub-Riemannian Geodesics in SE(2)

Erik Bekkers[1] (E.J.Bekkers@tue.nl), Remco Duits[1] (R.Duits@tue.nl),
Alexey Mashtakov[2] (A.Mashtakov@tue.nl), Gonzalo Sanguinetti[1] (g.r.sanguinetti@tue.nl)

Eindhoven University of Technology, The Netherlands

(1) (2) Funded by the European Union

Introduction

In computer vision it is common to extract salient curves via minimal paths or geodesics [1]. These geodesics minimize a length functional based on a cost function on the image domain that has a low value on locations with high curve saliency. Inspired by [2], we lift the image to extended domain $\mathrm{SE}(2) = \mathbb{R}^2 \rtimes S^1$ of positions and orientations, endowed with a *sub-Riemannian (SR)* metric. We present a wavefront propagation algorithm that finds SR-length minimizers in $\mathrm{SE}(2)$ with a metric tensor depending on a smooth external cost $\mathcal{C} : \mathrm{SE}(2) \to [\delta, 1]$, $\delta > 0$, computed from image data. First we compute the SR-distance map as a viscosity solution of a Hamilton-Jacobi-Bellman (HJB) system. Subsequent backward integration gives the SR-minimizers. Trackings in synthetic and retinal images show the advantage of including the SR-geometry.

Roto-Translations Group SE(2)

Lie group $\mathrm{SE}(2) = \mathbb{R}^2 \rtimes S^1 \ni (x, y, \theta) = g$ with operation

$$gg' = (\mathbf{X}, R_\theta)(\mathbf{X}', R_{\theta'}) = (R_\theta \mathbf{X}' + \mathbf{X}, R_{\theta+\theta'}),$$

where $\mathbf{X} = (x, y)$, and R_θ is a planar rotation over angle θ.
A moving frame of references:

$$\begin{aligned}
\mathcal{A}_1|_g &= \cos\theta\, \partial_x|_g + \sin\theta\, \partial_y|_g = (L_g)_* \,\partial_x|_e\,,\\
\mathcal{A}_2|_g &= \partial_\theta|_g = (L_g)_*\, \partial_\theta|_e\,,\\
\mathcal{A}_3|_g &= -\sin\theta\, \partial_x|_g + \cos\theta\, \partial_y|_g = (L_g)_*\, \partial_y|_e\,,
\end{aligned}$$

where $(L_g)_*$ is push-forward of left multiplication $L_g h = gh$.

Sub-Riemannian (SR) Structure

SR-manifold $(SE(2), \Delta, G^{\mathcal{C}})$, with
left-invariant distribution $\Delta = \mathrm{span}\{\mathcal{A}_1, \mathcal{A}_2\} \subset T(\mathrm{SE}(2))$ and
inner product $G^{\mathcal{C}}$ on Δ:

$$G^{\mathcal{C}}|_{\gamma(t)}(\dot\gamma(t), \dot\gamma(t)) = \mathcal{C}^2(\gamma(t)) \left(\xi^2 |\dot x(t) \cos\theta(t) + \dot y(t) \sin\theta(t)|^2 + |\dot\theta(t)|^2\right),$$

with $\gamma : \mathbb{R} \to \mathrm{SE}(2)$ a smooth curve, $\xi > 0$ constant, and
$\mathcal{C} : \mathrm{SE}(2) \to [\delta, 1], \delta > 0$ is a given external smooth cost.

SR-distance:

$$d(p, q) = \inf\{\int_0^T \sqrt{G^{\mathcal{C}}|_{\gamma(t)}(\dot\gamma(t), \dot\gamma(t))}dt \mid \gamma(0) = p, \gamma(T) = q, \dot\gamma(t) \in \Delta|_{\gamma(t)} \text{ a.e. in } [0, T]\}.$$

SR-minimizers are solutions to the optimal control problem

$$\dot\gamma = u^1\, \mathcal{A}_1|_\gamma + u^2\, \mathcal{A}_2|_\gamma\,,\ \gamma(0) = e,\ \gamma(T) = g,\ (u^1(t), u^2(t)) \in \mathbb{R}^2,$$

$$l(\gamma(\cdot)) = \int_0^T \mathcal{C}(\gamma(t)) \sqrt{\xi^2 |u^1(t)|^2 + |u^2(t)|^2}\, \mathrm{d}t \to \min.$$

Data-Driven SR-Geodesics

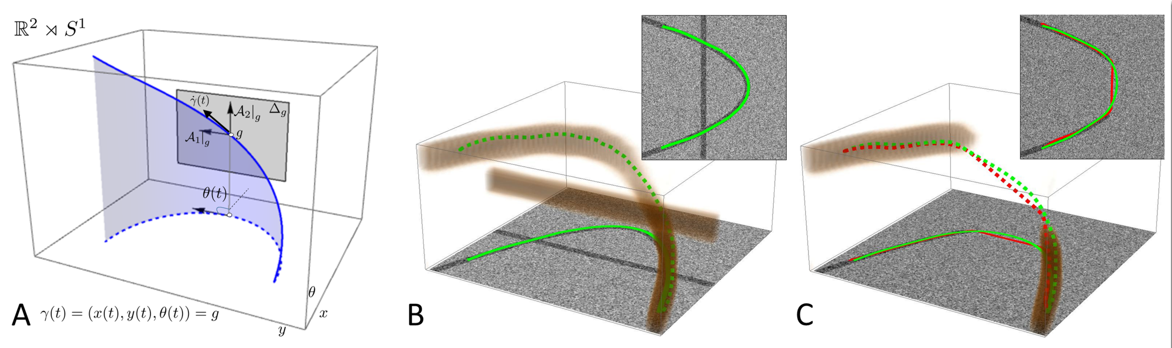

A: Every point of planar curve $\gamma_{2D}(t) = (x(t), y(t))$ is lifted to a point $g = \gamma(t) = (x(t), y(t), \theta(t)) \in \mathrm{SE}(2)$ of horizontal curve (solid line) by setting $\theta(t) = \arg(\dot x(t) + i\dot y(t))$. Then, tangent vectors $\dot\gamma(t) \in \Delta|_{\gamma(t)}$.
B: In $\mathrm{SE}(2)$ crossing structures are disentangled.
C: SR-geodesic (green) better follows curvilinear structure along the gap than Riemannian geodesic (red).

Wavefront Propagation

1. Compute SR-distance map.
2. Find SR-minimizers by steepest descent.

Denote by $W : SE(2) \to \mathbb{R}$ a SR-distance between given element $g \in \mathrm{SE}(2)$ and unit element $e = (0, 0, 0)$.

$$\text{HJB system} \begin{cases} \sqrt{\xi^{-2}|\mathcal{A}_1 W|^2 + |\mathcal{A}_2 W|^2} = \mathcal{C}, \\ W(e) = 0, \end{cases} \tag{1}$$

describes SR-wavefront propagation. When the wavefront intersect itself a geodesic is not longer a SR-minimizer (it loses optimality). By imposing a viscosity condition, our method produces the part of the wavefront before self intersection.

Theorem 1 (New)

Let $W(g)$ be the viscosity solution of (1). Then the iso-contours $\mathcal{S}_t = \{g \in SE(2) \mid W(g) = t\}$ are geodesically equidistant with unit speed. A SR-geodesic is found by backward integration

$$\begin{cases} \dot\gamma = -\frac{1}{\mathcal{C}^2}\left(\frac{1}{\xi^2}\mathcal{A}_1 W(\gamma)\, \mathcal{A}_1|_\gamma + \mathcal{A}_2 W(\gamma)\, \mathcal{A}_2|_\gamma\right), \\ \gamma(0) = g. \end{cases} \tag{2}$$

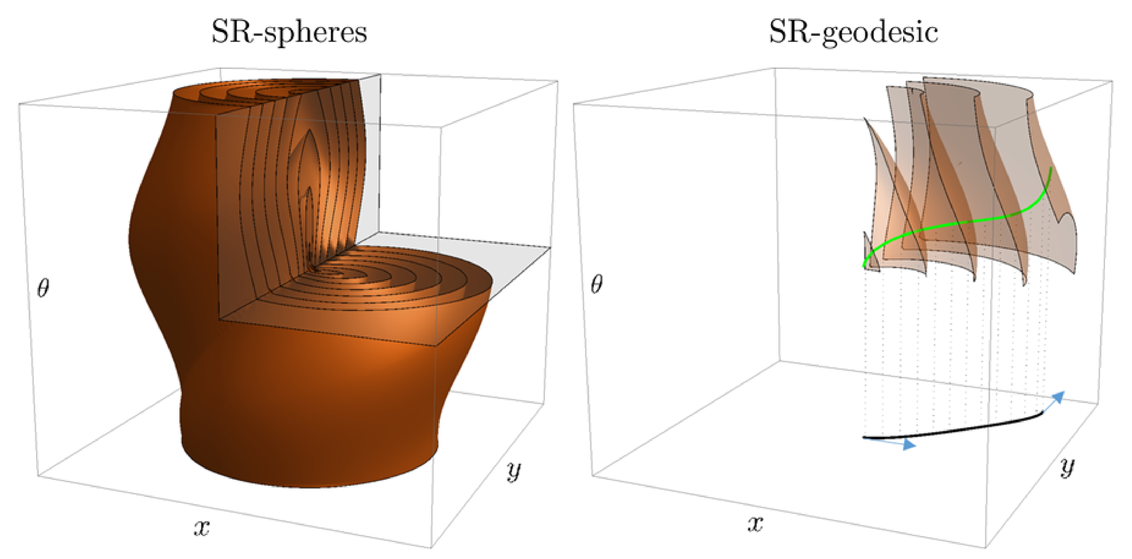

Theorem 2 (New)

Let $W(g)$ be the viscosity solution of (1) with $\mathcal{C}(g) \equiv 1$. Then:
- $\mathcal{S}_t$ equals the **SR-sphere** of radius t,
- backward integration (2) gives **optimal** geodesics reaching e at $t = d(g, e)$.

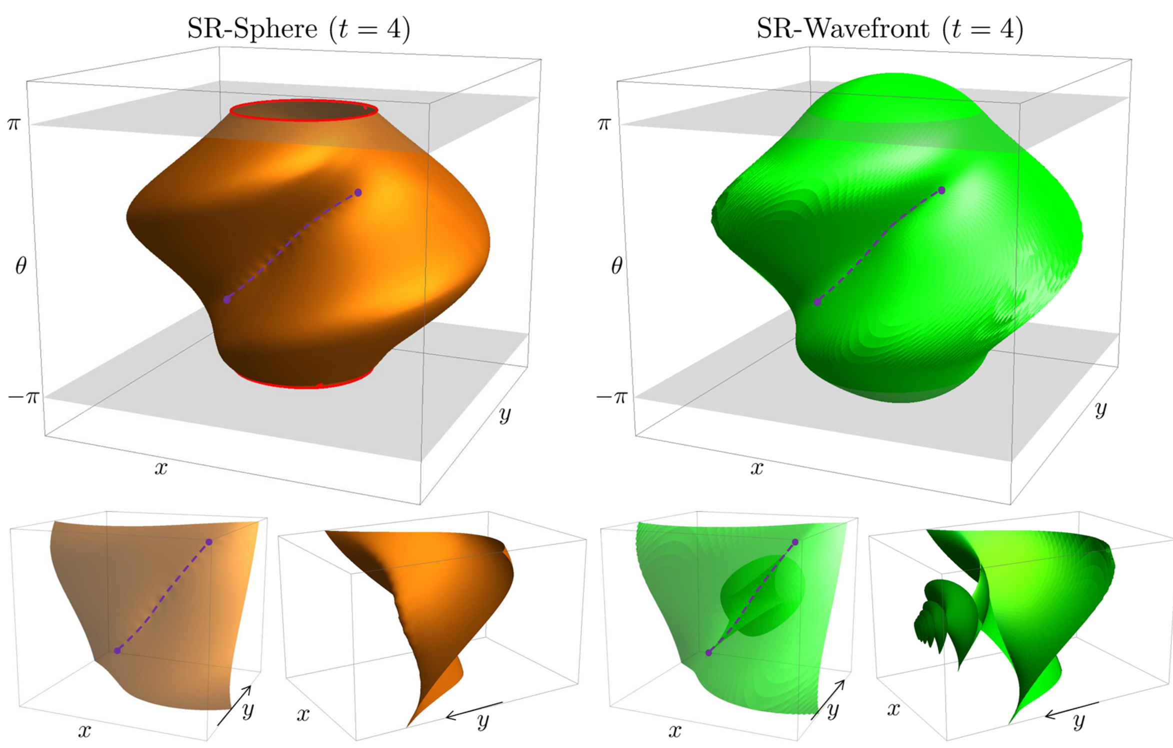

Implementation

We resort to subsequent auxiliary initial value problems (IVP) on $\mathrm{SE}(2)$, and obtain the solution of (1) via:

$$W(g) = \lim_{\epsilon \to 0} \lim_{n \to \infty} W^{\epsilon}_{n+1}(g, (n+1)\epsilon),$$

where W^{ϵ}_{n+1} satisfies IVP for HJB-equation, explained in SSVM paper, and more detailed in [8].

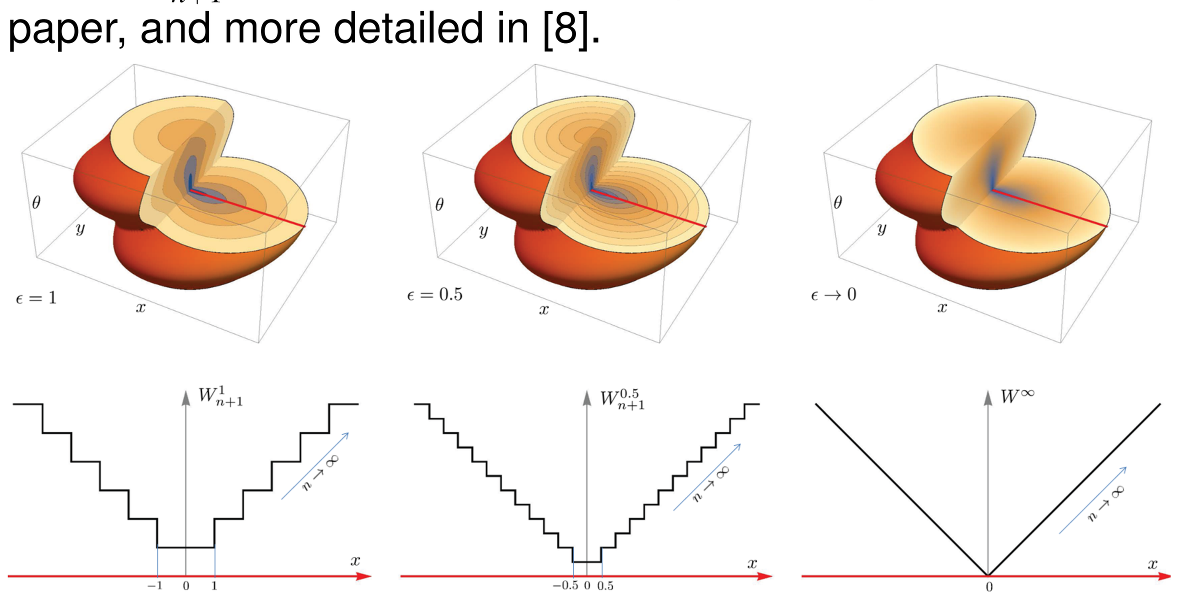

New Fast Marching [6] implementation to appear in [7].

Validation for Uniform Cost $\mathcal{C} \equiv 1$

A 1st Maxwell point is a point where two distinct geodesics meet for the first time with equal length (and lose optimality)

$$\exists \tilde\gamma(t) - \text{geod.}\ : \gamma(t) \not\equiv \tilde\gamma(t), \gamma(0) = \tilde\gamma(0), \gamma(T) = \tilde\gamma(T).$$

All 1st Maxwell points form the 1st Maxwell set. Comparison with exact 1st Maxwell set, obtained in [5], verifies our novel PDE method. The advantage of our PDE approach is that it extends also to $\mathcal{C} \not\equiv 1$. The Maxwell set can be computed by:

$$\mathcal{M}_{num} = \bigcup_{i=1}^{2} \{(x, y, \theta) \in SE(2) \mid \mathcal{A}_i^{+} W(x, y, \theta) > 0,\ \mathcal{A}_i^{-} W(x, y, \theta) < 0\}.$$

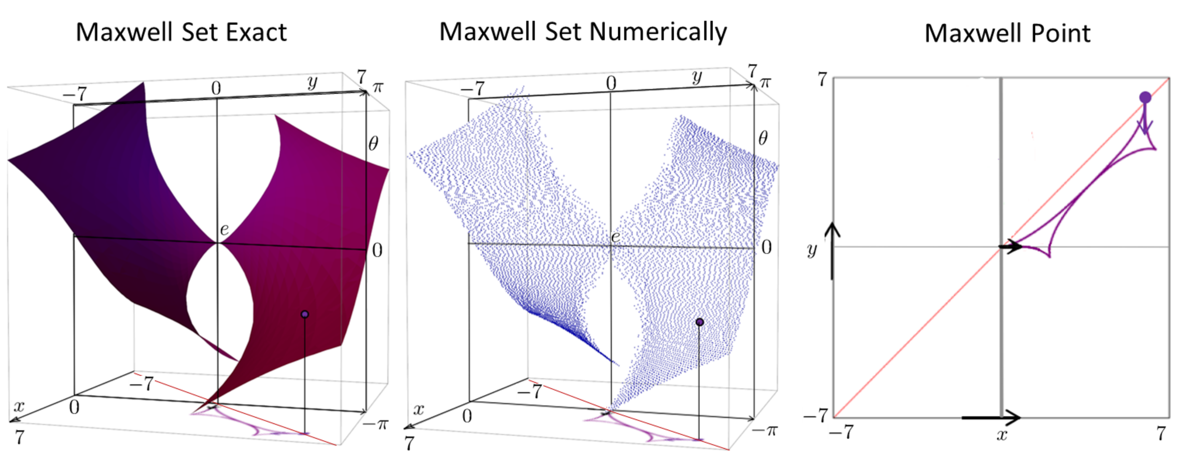

Application in Retinal Imaging

The retinal vasculature enables non-invasive observation of the human circulatory system. A variety of eye-related and systematic diseases such as glaucoma, diabetes, hypertension etc, affect the vasculature and may cause functional or geometric changes. Automated quantification of these defects promises massive screening for vascular diseases on the basis of fast retinal photography. Prior to the diagnosis, the full vascular tree must be detected.

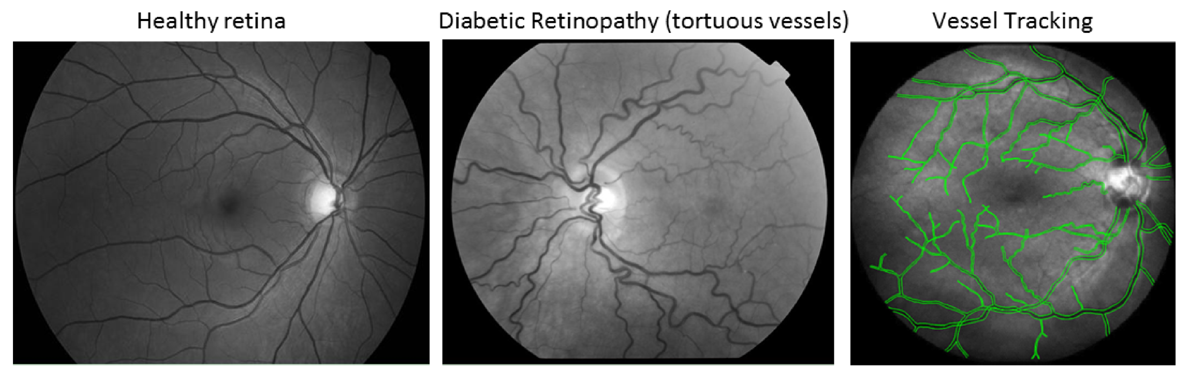

Construction of External Cost

Typical problems that arise are crossing and bifurcation of vessels, and their high curvature. To avoid these problems we lift the image to extended domain $\mathrm{SE}(2)$ of positions and orientations, endowed with a sub-Riemannian (SR) metric. Local optimization problem for vessel tracking in $\mathrm{SE}(2)$ is proposed in [4]. We improve this, by considering a global optimization. This allows us to track a vascular network in an optimal way. Based on image $f(x, y)$ define external cost $\mathcal{C}(x, y, \theta)$ via invertible Orientation Scores in $\mathrm{SE}(2)$ [3].

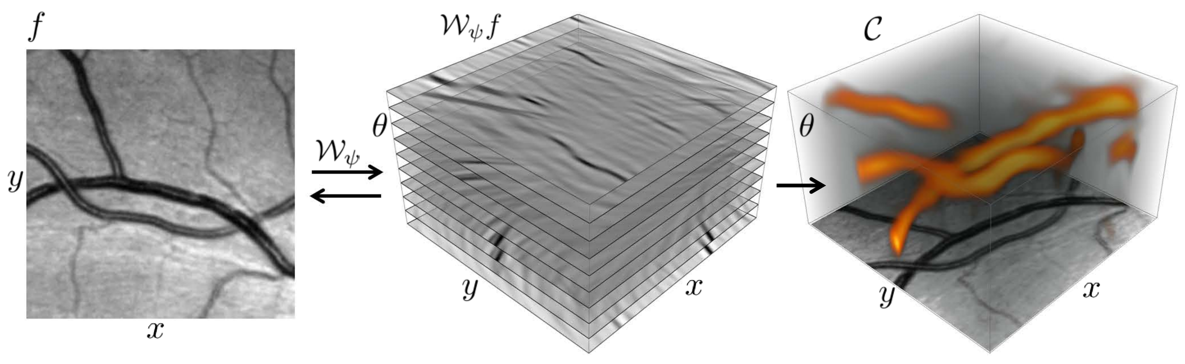

Results

As a feasibility study for the application of our method in retinal images we tested the method on many image patches exhibiting crossings, bifurcations, and low contrast.
We compared to wavefront propagation methods based on a data-adaptive Riemannian metric on $\mathbb{R}^2$, and a data-adaptive Riemannian metric on $\mathrm{SE}(2)$. The advantage of including the sub-Riemannian geometry is clear. The advantage of our approach over previous work on automated vascular tree detection [4] is that each curve is a global minimizer of a formal geometric control curve optimization problem.

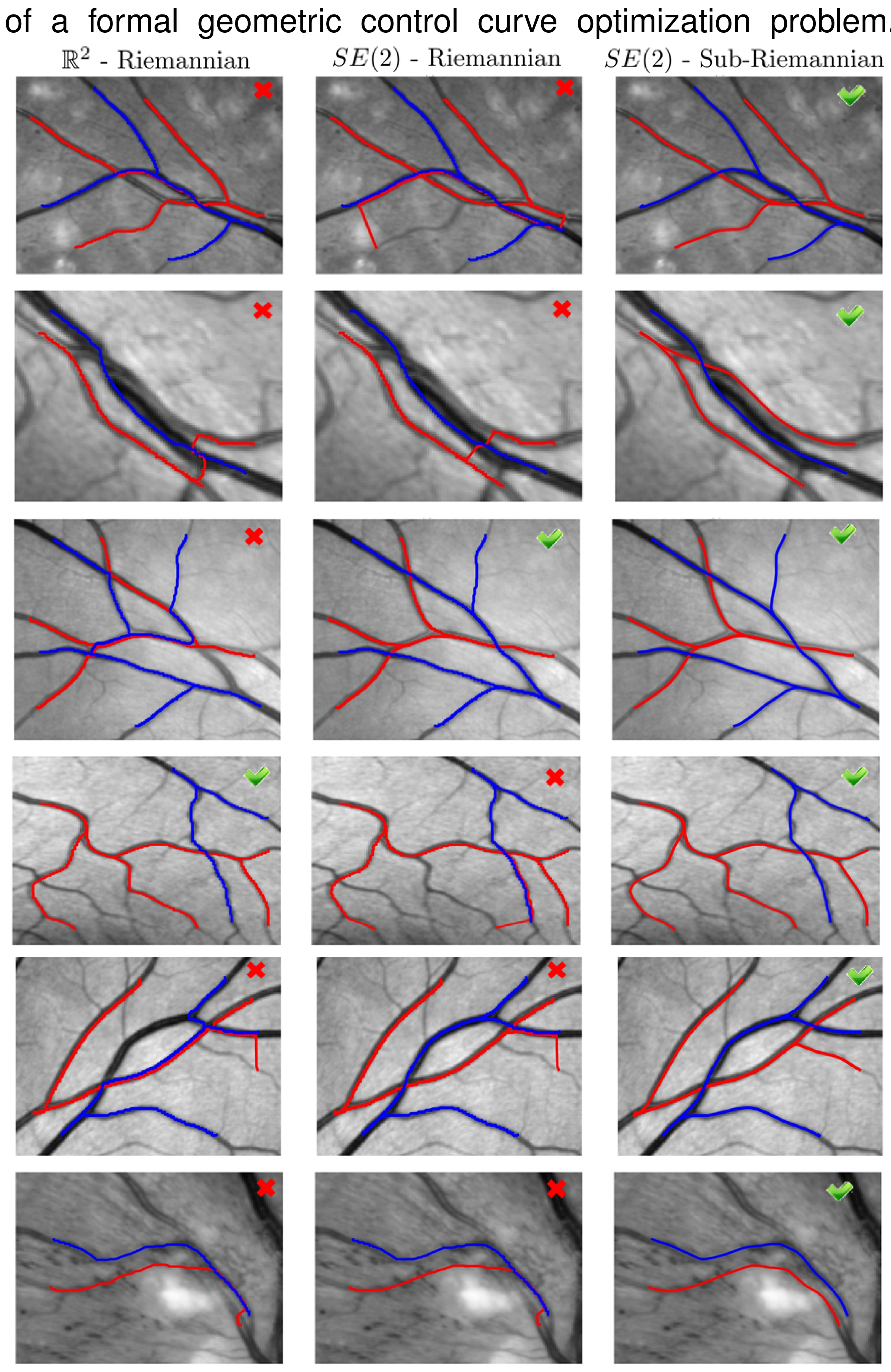

More: `www.bmia.bmt.tue.nl/people/RDuits/Bekkersexp.zip`

Bibliography

[1] G. Peyré, M. Péchaud, R. Keriven, L.D. Cohen, *Geodesic methods in computer vision and graphics*, FTCCGV, 2010. **[2]** G. Citti, A. Sarti, *A cortical based model of perceptual completion in the roto-translation space*, JMIV, 2006. **[3]** R. Duits, M. Felsberg, G. Granlund, B.H. Romeny, *Image Analysis and Reconstruction using a Wavelet Transform Constructed from a Reducible Representation of the Euclidean Motion Group*, IJCV, 2007. **[4]** E. Bekkers, R. Duits, T. Berendschot, B.H. Romeny, *A Multi-Orientation Analysis Approach to Retinal Vessel Tracking*, JMIV, 2014. **[5]** I. Moiseev, Y. L. Sachkov, *Maxwell strata in sub-Riemannian problem on the group of motions of a plane*, ESAIM: COCV, 2010. **[6]** J-M. Mirebeau, *Anisotropic Fast-Marching on cartesian grids using Lattice Basis Reduction*, SIAM JNA, 2014. **[7]** G. Sanguinetti, R. Duits, E. Bekkers, M. Janssen, A. Mashtakov, J-M. Mirebeau, *Sub-Riemannian Fast Marching in* $\mathrm{SE}(2)$, Submitted to CIARP, 2015. **[8]** E.J. Bekkers, R. Duits, A. Mashtakov and G.R. Sanguinetti, *A PDE Approach to Data-driven Sub-Riemannian Geodesics in* $\mathrm{SE}(2)$, Submitted to SIIMS, 2015.